Simplified Constitutive Model for Simulation of Cyclic Response of Shallow Foundations: Validation against Laboratory Tests

I. Anastasopoulos[1]; F. Gelagoti[2]; R. Kourkoulis[3]; and G. Gazetas, M.ASCE[4]

Abstract: The nonlinear response of shallow foundations has been studied experimentally and analytically. However, the engineering community is not yet convinced of the applicability of such concepts in practice. A key prerequisite is the ability to realistically model such effects. Although several sophisticated constitutive models are readily available in the literature, their use in practice is limited, because (1) they typically require extensive soil testing for calibration; (2) as they are implemented in highly specialized numerical codes, they are usually restricted to simple superstructures; and (3) in most cases, they can only be applied by numerical analysis specialists. Attempting to overcome some of these difficulties, this paper develops a simplified but fairly comprehensive constitutive model for analysis of the cyclic response of shallow foundations. On the basis of a kinematic hardening constitutive model with Von Mises failure criterion (readily available in commercial finite element codes), the model is made pressure sensitive and capable of reproducing both the low-strain stiffness and the ultimate resistance of clays and sands. Encoded in ABAQUS through a simple user subroutine, the model is validated against (a) centrifuge tests of shallow footings on clay under cyclic loading and (b) large-scale tests of a square footing on dense and loose sand under cyclic loading, conducted in the European Laboratory for Structural Analysis for the TRISEE project. The performance of the model is shown to be quite satisfactory, and discrepancies between theory and experiment are discussed and potential culprits are identified. Requiring calibration of only two parameters and being easily implemented in commercial FE codes, the model is believed to provide an easily applicable engineering solution. **DOI: 10.1061/(ASCE)GT.1943-5606.0000534.** *© 2011 American Society of Civil Engineers.*

CE Database subject headings: Shallow foundations; Numerical analysis; Constitutive models; Load bearing capacity; Centrifuge; Experimentation; Validation; Laboratory tests.

Author keywords: Rocking foundation; Numerical method; Constitutive relations; Bearing capacity; Cyclic response; Centrifuge experiments; Experimental validation.

Introduction

The fundamental problem that has motivated the study in this paper is the seismic response of slender foundation—structure systems, for which P-Δ effects play a significant role. Under severe seismic shaking, the shallow foundations of these systems may experience detachment from the supporting soil because of the large overturning moments (arising from inertial and gravitational forces). The ensuing rotational uplift will, in most cases, lead to a large increase of the imposed stresses on the soil under the edge of the footing. Mobilization of bearing-capacity failure mechanism under the action of combined moment-shear-vertical, $M - Q - N$, loading is a possible outcome.

The occurrence of such an event does not necessarily imply failure, thanks to the cyclic and kinematic nature of the seismic excitation. As a result of the cyclic character of the motion, a bearing-capacity failure mechanism may lead to only a small rotation before the direction of motion is reversed. If the next pulse of the ground motion is also strong, another bearing-capacity failure mechanism will develop on the opposite side of the foundation, and so on, until the end of shaking.

The kinematic character of seismic shaking (i.e., the loading in the form of dynamic displacement imposed at the base) distinguishes it from external loading in the form of force applied to the mass. Even if the base acceleration is larger than the critical (yield) acceleration A_c, the acceleration that develops in the mass cannot exceed A_c, and failure is not necessarily the consequence.

Performance-based design in earthquake geotechnics (i.e., design on the basis of limiting the maximum and permanent displacements and rotations of our facilities during the design earthquake) has its justification in the above consequences of the cyclic and kinematic character of motion. Thus, the concept of allowing significant foundation uplifting (implying a geometric nonlinearity) and mobilization of ultimate bearing-capacity (implying material inelasticity) during strong shaking (Fig. 1) has been suggested in recent years as a change from the prevailing conventional design philosophy (e.g., FEMA 2000). In fact, a growing body of evidence suggests that allowing such nonlinear-inelastic foundation response is not only unavoidable, but may even be beneficial (Paolucci 1997; Pecker 1998, 2003; Martin and Lam 2000; Makris and Roussos 2000; Comartin et al. 2000; Pecker and Pender 2000; Faccioli et al. 2001; Kutter et al. 2003; Gazetas et al. 2003; 2007; Gajan et al. 2005; Paolucci et al. 2008; Kawashima et al. 2007;
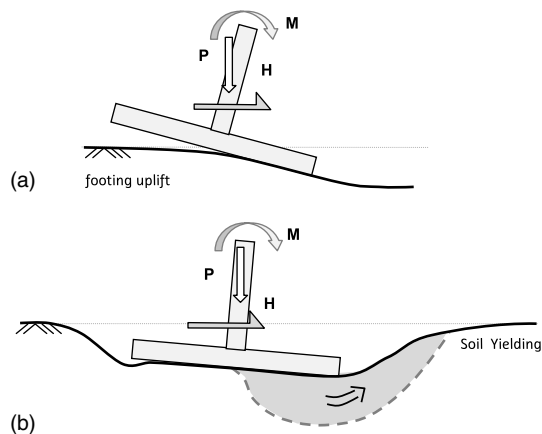
Fig. 1. Mobilization of the ultimate capacity of the soil-foundation system. Schematic of a foundation subjected to combined horizontal and vertical loading and bending moment: (a) when uplifting is critical; (b) when the bearing-capacity failure mechanism is prevailing

Gajan and Kutter 2008; Chatzigogos et al. 2009; Anastasopoulos et al. 2009).

Although the nonlinear load-displacement response of shallow foundations has been extensively studied (e.g., Bartlett 1979; Taylor et al. 1981; Georgiadis and Butterfield 1988; Butterfield and Gottardi 1994; Faccioli et al. 2001; Gajan et al. 2005; Kutter 1995; Houlsby and Puzrin 1999; Allotey and El Naggar 2003; 2008; Pecker 2005; Harden et al. 2005; Pender 2007; Gajan and Kutter 2008; Harden and Hutchinson 2009), there is still quite a long way before such a major change in seismic design philosophy could be applicable in practice. Aside from reliability issues, a key prerequisite to render such concepts more attractive to engineers is the capability to realistically model the inelastic response of foundations.

Although several advanced and sophisticated constitutive models have appeared in the literature (e.g., Prevost 1980; Dafalias 1986; Houlsby 1986; Jefferies 1993; Gajo and Wood 1999; Pestana 1994; Pestana and Whittle 1995; 1999; Jeremic et al. 1999; Puzrin and Houlsby 2001a, b, c; Einav et al. 2003; Dafalias and Manzari 2004; Houlsby and Puzrin 2006), the current state of the art in nonlinear analysis of foundations emphasizes the development of macroelement models (Paolucci 1997; Cremer et al. 2001, 2002; Le Pape and Sieffert 2001; Pecker 2002; Paolucci et al. 2008). Macroelement models are emphasized not only because sophisticated constitutive models typically require extensive calibration of their numerous parameters, but also because their use is also restricted to simple superstructures as they are usually implemented in highly specialized finite element (FE) or finite differences (FD) codes. Additionally, in most cases, such models can only be applied by numerical analysis specialists, prohibiting their use in practice. In contrast, macroelements constitute a valid solution, but are also usually restricted (at least until today) to simple superstructures.

In an attempt to overcome some of the above difficulties, this paper presents a simplified constitutive model for analysis of the cyclic response of shallow foundations. The model is based on a simple kinematic hardening constitutive model with Von Mises failure criterion, available in commercial FE codes. As discussed in the sequel, following a simplified procedure the model is modified to be applicable for sand, and is encoded in the FE code ABAQUS through a simple user subroutine, hence formulating a numerical tool able to provide a fully coupled solution to soil-structure interaction problems such as the ones examined in this paper. The model

is validated against centrifuge tests performed at UC Davis and large-scale 1-g experiments under the EU program TRISEE. Despite its simplicity and lack of generality and rigor, for the particular type of problem investigated herein such a constitutive model yields quite reasonable results. Requiring calibration of only two parameters, and being (relatively) easy to implement in a commercial FE code, the developed model is believed to provide a practically applicable solution. By no means should this model be considered a general purpose model, able to reproduce all aspects of complex soil behavior under static and dynamic loading. However, despite its limitations (discussed in the sequel), this model may be used to model different aspects of dynamic soil response.

Constitutive Relations

As previously discussed, the constitutive model presented herein is based on a rather simple kinematic hardening model with Von Mises failure criterion, which is available in ABAQUS. On the basis of the work of Armstrong and Frederick (1966), the original model (Lemaitre and Chaboche 1990) may be considered appropriate for clay, the behavior of which under undrained conditions is considered as normal-pressure-independent. Of course, phenomena such as pore-pressure buildup and dissipation cannot possibly be captured. However, for the key aspects of the investigated problem, given the rapid application of seismic loading, the undrained behavior is considered a reasonable simplification of reality. As described in the sequel, the model is modified, to be applicable for sands as well. To provide a more concise presentation, the relevant constitutive relations for clay and sand are discussed together.

An extended pressure-dependent Von Mises failure criterion [Fig. 2(a)] is combined with nonlinear kinematic hardening and the associated plastic flow rule. This assumption is not valid for sand, the volumetric behavior of which largely depends on dilation. The evolution of stresses is defined as

$$\sigma = \sigma_o + \alpha \tag{1}$$

where σ_o = the stress at zero plastic strain and α = "backstress." The latter determines the kinematic evolution of the yield surface in the stress space. This is performed through a function F that defines the yield surface:

$$F = f(\sigma - \alpha) - \sigma_o \tag{2}$$

where $f(\sigma - \alpha)$ = equivalent Mises stress with respect to the backstress α.

Given the associated plastic flow, the plastic flow rate is $\dot{\varepsilon}^{pl}$

$$\dot{\varepsilon}^{pl} = \dot{\bar{\varepsilon}}^{pl} \frac{\partial F}{\partial \sigma} \tag{3}$$

where $\dot{\bar{\varepsilon}}^{pl}$ = equivalent plastic strain rate.

The evolution of stress is composed of two components:
1. An isotropic hardening component, which describes the change in the equivalent stress defining the size of the yield surface σ_o as a function of plastic deformation, and
2. A nonlinear kinematic hardening component, which describes the translation of the yield surface in the stress space, and is defined by the superposition of a purely kinematic term and a relaxation term (that introduces the nonlinear behavior).

The isotropic hardening component defines the evolution of the size of the yield surface as a function of the equivalent plastic strain $\bar{\varepsilon}^{pl}$

$$\sigma_o = \sigma_0 + Q_\infty(1 - e^{-b\bar{\varepsilon}^{pl}}) \tag{4}$$
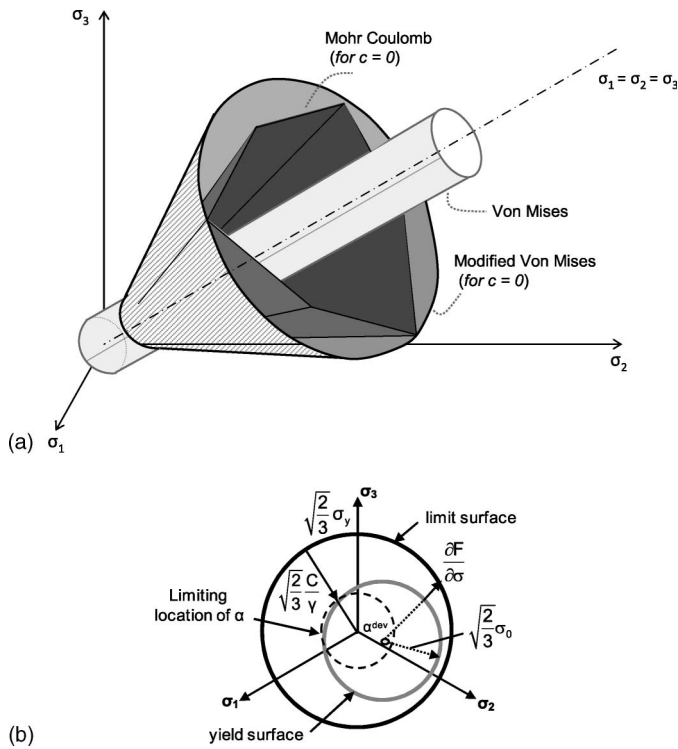
Fig. 2. Simplified constitutive model: (a) representation of the extended pressure-dependent Von Mises failure criterion in the principal stress space (hashed shape) together with the Von-Mises (light grey shape) and the Mohr Coulomb failure criterion (dark grey shape); (b) projection of the failure surface at pressure $p = (\sigma_1 + \sigma_2 + \sigma_3)/3$ on the π-plane

where Q_∞ and b are model parameters, defining the maximum change of the size of the yield surface and the rate of this change with $\bar{\varepsilon}^{pl}$, respectively. For $Q_\infty = 0$, the size of the yield surface remains constant and the model reduces to a nonlinear kinematic hardening model.

The evolution of the kinematic component of the yield stress is described by the expression

$$\dot{\alpha} = C\frac{1}{\sigma_o}(\sigma - \alpha)\dot{\bar{\varepsilon}}^{pl} - \gamma\alpha\dot{\bar{\varepsilon}}^{pl} \qquad (5)$$

where C = initial kinematic hardening modulus [$C = \sigma_y\varepsilon_y = E = 2(1 + \nu)G_o$] and γ is a parameter determining the rate of decrease of the kinematic hardening with increasing plastic deformation. The preceding equation is based on Ziegler's (1959) kinematic hardening law, in which the "recall" term $\gamma\alpha\dot{\bar{\varepsilon}}^{pl}$ has been added to introduce the nonlinearity in the evolution law (Lemaitre and Chaboche 1990). Fig. 2(b) illustrates the evolution of the two hardening components (kinematic and isotropic) for multiaxial loading. According to the evolution law governing the kinematic hardening component, the "backstress" α must be contained within a cylinder of radius $\sqrt{2/3}C/\gamma$. The bounding of the yield surface demands that all stress points lie within a cylinder of radius $\sqrt{2/3}\sigma_\gamma$, where σ_γ is the maximum yield stress at saturation. At large plastic strains, when σ approaches σ_y, the magnitude of α becomes equal to $\alpha_s = C/\gamma$ and $(\sigma - \alpha)$ tends to σ_o [Fig. 3(a)], which means that $\dot{\alpha}$[Eq. (5)] tends to zero.

For the case of clays, the undrained strength of which is not pressure dependent, the maximum yield stress can be defined as
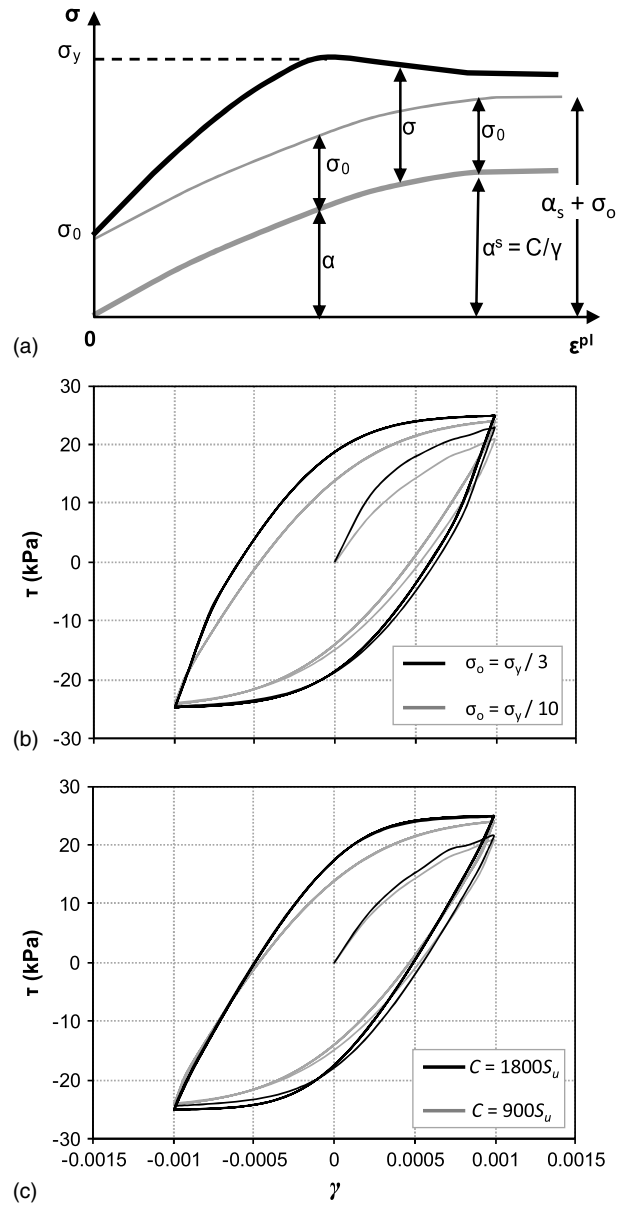
$$\sigma_y = \sqrt{3}S_u \qquad (6)$$

Fig. 3. (a) Parameters incorporated into the formulation of the constitutive model, and example illustration of model sensitivity to (b) parameter σ_o (which controls the onset of inelasticity); and (c) parameter C (i.e., the initial Young's modulus, which controls the initial stiffness)

Since $\sigma_y = c/\gamma + \sigma_0$, parameter γ can be expressed as (Gerolymos et al. 2005)

$$\gamma = \frac{C}{\sqrt{3}S_u - \sigma_0} \qquad (7)$$

In the case of sand, the shear strength depends on the confining pressure and the friction angle φ. This pressure-dependency is incorporated in the model by defining the yield stress at saturation as a function of octahedral stress and the friction angle, as follows:

$$\sigma_y = \sqrt{3}\left(\frac{\sigma_1 + \sigma_2 + \sigma_3}{3}\right)\sin\varphi \qquad (8)$$

where σ_1, σ_2, and σ_3 represent the principal stresses. Accordingly, parameter γ can be expressed as

$$\gamma = \frac{C}{\sqrt{3}\left(\frac{\sigma_1+\sigma_2+\sigma_3}{3}\right)\sin\varphi - \sigma_0} \quad (9)$$

Parameter σ_0, which controls the initiation of the nonlinear behavior, is defined as a fraction λ (typically ranging from 0.1–0.3) of the yield stress σ_y:

$$\sigma_0 = \lambda\sigma_y \quad (10)$$

Fig. 3(a) summarizes the parameters incorporated in the formulation of the proposed model, whereas Fig. 3(b) vividly illustrates the effect of σ_o on material behavior (in terms of shear stress-shear strain loops) for two extremes. For $\sigma_o = 0.1\sigma_y$, the material exhibits nonlinear behavior even for very low amplitude strains. In contrast, for $\sigma_o = 0.3\sigma_y$, a considerable amount of shear strain is necessary to enter the nonlinear regime. To clarify, the model as presented herein does not account for strain softening. Yet, in Fig. 3(a) the more general case of strain softening soil is schematically illustrated just to define model parameters.

Parameter C is the Young's modulus for very small strains; it determines the initial "elastic" stiffness at low-strain amplitudes [Fig. 3(c)]. It can be directly computed on the basis of the measured shear wave velocity V_s, or estimated from empirical correlations (e.g., Hardin and Richart 1963; Robertson and Campanella 1983a, b; Seed et al. 1986; Mayne and Rix 1993) and expressed as a function of the overburden stress σ_y:

$$C = a\sigma_y \quad (11)$$

On the basis of such empirical correlations, the ratio a typically ranges from 150–1,000 (i.e., $E = 300S_u$ to $1,800S_u$) for clays and from 1,000 to 10,000 for sands.

The modified kinematic hardening constitutive model is encoded in the ABAQUS finite element environment through a user-defined subroutine. As already alluded to, model parameters can be easily calibrated, even with limited experimental or field data. In summary, the calibration requires the following data: (1) soil strength: S_u for clay, φ for sand; (2) small-strain stiffness: G_o or V_s (if measurement is not available, the aforementioned empirical correlations can be utilized); and (3) G-γ curves: to calibrate parameter λ and the ratio a.

For the purposes of the present study, model parameters were systematically calibrated for various levels of the overburden stress (for sands) and PI ratios (for clays), according to the experimental G-γ curves of Ishibashi a Zhang (1993) (see also Vucetic and Dobry 1991). To this end, a numerical simulation of the cyclic simple shear test was conducted. Fig. 4 portrays typical comparisons between experimental and computed G-γ and ξ-γ curves for sand. For the soil materials investigated herein, $\lambda = 0.1$ was found to provide a reasonable fit to G-γ curves. For lower confining pressures [Fig. 4(a)], the model slightly underpredicts the strength reduction at low to intermediate strains. The agreement is improved with increasing σ_{vo} [Fig. 4(b)]. As also seen in the FE-computed τ-γ (shear stress-shear strain) hysteresis loops of Fig. 5 (corresponding to a typical sand), because of the adoption of the Masing criterion for loading-unloading, the model overestimates the hysteretic damping for large shear strain amplitudes ($\gamma \approx 10^{-2}$). As expected, the reduction of λ leads to improvement of model accuracy. However, since σ_0 essentially defines the initiation of nonlinear soil behavior, a large reduction in λ unavoidably leads to an increase in computational cost. Therefore, an initial sensitivity analysis was performed to estimate the optimum range of λ, which was found to be between 0.1 and 0.3. The results presented herein refer to $\lambda = 0.1$ (or $\sigma_0 = 0.1\sigma_y$). Increasing λ to 0.3 leads to a 10% deviation from the presented results. Similarly, the value of a was

calibrated to more effectively capture the initial part of the stress-strain curve.

Model Validation for Clay

We first validate the original constitutive model for clay, making use of published UC Davis experimental results.

Description of Tests

Gajan et al. (2005) conducted experiments in the 9.1 m radius beam centrifuge at the Center of Geotechnical Modeling of the Univ. of California, Davis. The tests were conducted at 20 g centrifugal acceleration, comprising 40 models of shear wall footings imposed to cyclic and dynamic loading. A comprehensive set of footing dimensions, depths of embedment, dead load, initial factor of safety against static bearing-capacity failure, soil density, and soil types (dry sand and saturated clay) were parametrically investigated with respect to the nonlinear load-deformation foundation response. Four series of tests were conducted on dry sand ($D_r \approx 80\%$ and 60%) and one on saturated clay of $S_u \approx 100$ kPa. The latter is selected for model validation.

The structure had a weight of 364.8 kN, corresponding to an initial vertical factor of safety $FS_V = 2.8$. The footing length was $L = 2.672$ m and its width $B = 0.686$ m (all dimensions in prototype scale). The footing models were tested on a soil bed prepared in a rigid container. The material composing the clay layer consisted of remolded San Francisco Bay Mud, with Atterberg limits $LL = 90$ and $PL = 38$. Before spinning, the mud was consolidated on top of a dense sand layer. The final thickness of the consolidated clay layer was 1.7 m.

Fig. 6 displays the centrifuge model setup and the relevant instrumentation (for the tests investigated here: vertical push and slow cyclic lateral push). Each test series included at least one concentric vertical push test to measure the bearing capacity of the soil and to confirm the undrained shear strength of the clay. This initial test was displacement-controlled to mobilize the foundation capacity without developing excessive movement.

The vertical push was followed by slow cyclic lateral push tests, during which displacement was applied through an actuator at a height of 4.75 m from the footing (close to the height of the center of gravity of the structure). The height of the structure tested was 10 m. Displacement was applied in packets of increasing amplitude, each one including three cycles of constant amplitude. Horizontal and vertical linear potentiometers were mounted at different positions on the wall and the footings to measure the displacements of the structure; a load-cell attached on the actuator was measuring the force acting upon the wall. A detailed description of the experiments and the procedures followed are documented in Rosebrook and Kutter (2001a, b, c), Gajan et al. (2003a, b), Kutter et al. (2003), and Phalen (2003).

Methodology of Numerical Analysis

The problem is analyzed through three-dimensional (3D) finite element (FE) analysis. Fig. 7 displays the developed 3D FE model, which takes advantage of centrifuge model symmetry. The soil is modeled with eight-noded hexahedral continuum elements. The same elements are used for the foundation. In contrast to the soil, their behavior is assumed linear elastic, and they are given the Young's modulus of aluminum (used in the centrifuge model tests). An initial sensitivity analysis revealed that the footing has to be discretized into at least 10 elements to reproduce the mechanism of bearing-capacity failure (for the vertical loading test) and the rocking behavior (for the lateral cyclic pushover test). The
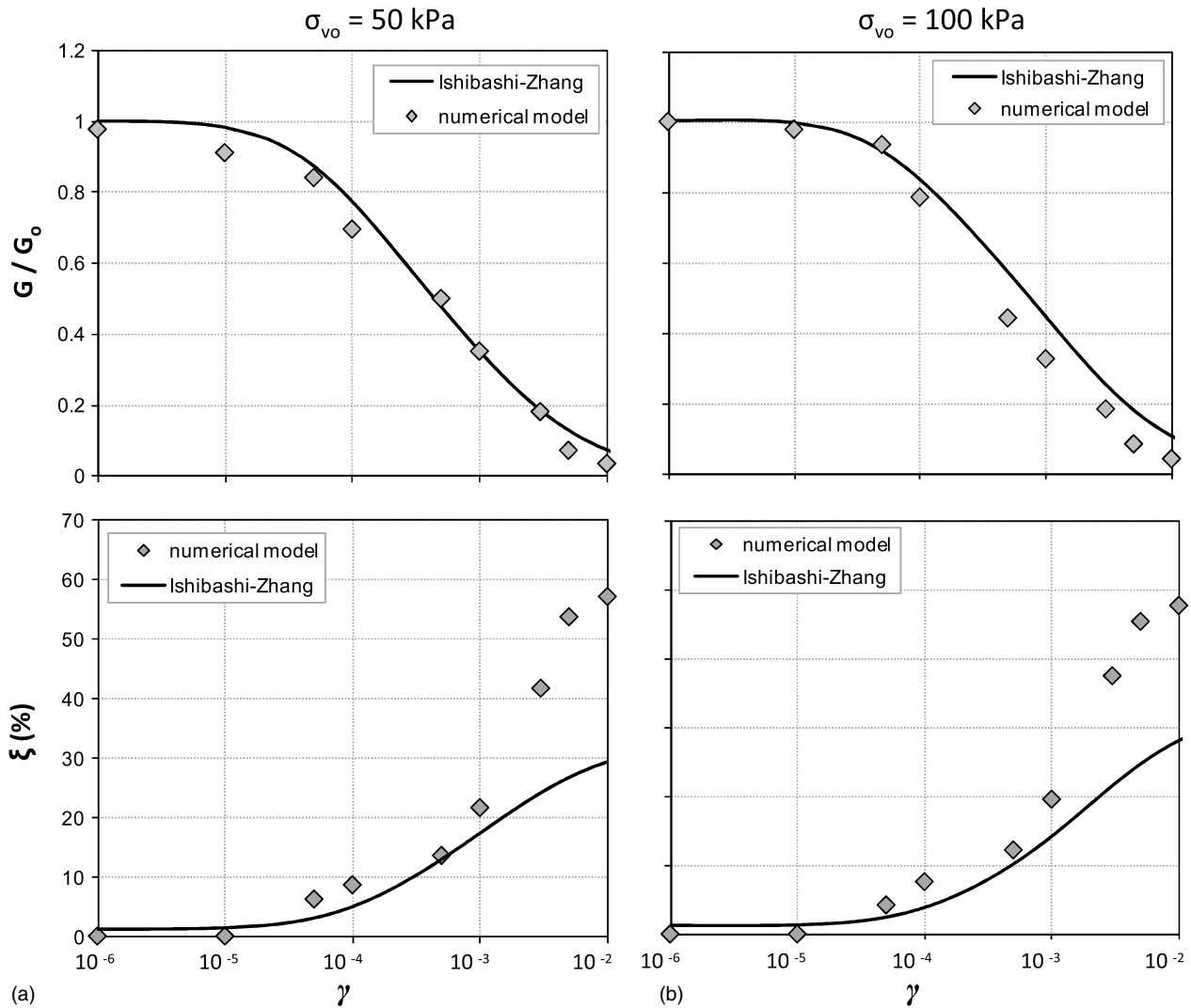
Fig. 4. Constitutive model calibration for sand. Comparison of FE-computed $G - \gamma$ and $\xi - \gamma$ curves with published curves of Ishibashi and Zhang (1993) for three levels of confining pressure: (a) $\sigma_{vo} = 50$ kPa; (b) $\sigma_{vo} = 100$ kPa

soil-foundation interface is modeled using special "gap" elements (ABAQUS), which allow the structure to slide on or detach from the soil depending on the loading. These elements connect the nodes of the soil with the corresponding nodes (i.e., having the same coordinates) of the foundation, which are initially in contact but are allowed to separate when uplifting takes place. While being "infinitely" stiff in compression, the gap elements are tensionless, allowing separation. In the horizontal direction, they follow Coulomb's friction law, allowing for sliding when the friction force is exceeded. In the analyses presented herein, the friction coefficient was set to 0.7. The shear wall was modeled with practically rigid three-dimensional beam elements. Since the response is governed by foundation rocking, the flexural deformation of the shear wall may be assumed to be negligible. Hence, no attempt was made to model accurately the shear wall. Nonlinear P-δ geometry effects were also taken into account.

Soil stiffness has been assumed to be constant with depth, which is a fair assumption for OC clays. In the absence of V_s or G_o measurements, parameter C (i.e., the initial stiffness) of our constitutive model was calibrated to exploit the results of vertical push tests. Keeping all other parameters constant ($S_u = 100$ kPa, Poisson's ratio $\nu = 0.49$), C was parametrically varied from $300S_u$ to $1{,}800S_u$. The best fit was achieved for $C = E = 600S_u$, which

was adopted for the analysis of the slow cyclic lateral sequence. No further calibration was conducted with respect to parameters λ and α, as the already conducted calibration results for $PI = 50$ clay were utilized (Table 1). Fig. 8 illustrates the comparison between the FE-computed ultimate vertical load and the experimental load-displacement curves (as measured by the two potentiometers on the footing) for the vertical loading.

The FE-computed bearing-capacity under undrained conditions was $p_{ult} = 560$ kPa, which corresponds to a static factor of safety $FS_v = 2.87$. This compares satisfactorily with the experimentally measured bearing-capacity $p_{ult} = 546$ kPa (i.e., $FS_v = 2.8$) and is, understandably, slightly higher than the theoretical Prandtl (1921) solution for plane-strain:

$$p_{ult} = (\pi + 2)S_u = 514 \text{ kPa} \qquad (12)$$

Having partially calibrated our model using the results of the vertical push test (parameter C only), we now proceed to the simulation of the slow cyclic lateral pushover sequence. The FE model was subjected to three displacement-controlled loading packets (each one consisting of three load cycles) of increasing amplitude. Loading during the experiment was applied slowly, with the period of each cycle being equal to 200 s. In the numerical simulation, the displacement was applied quasi-statically.
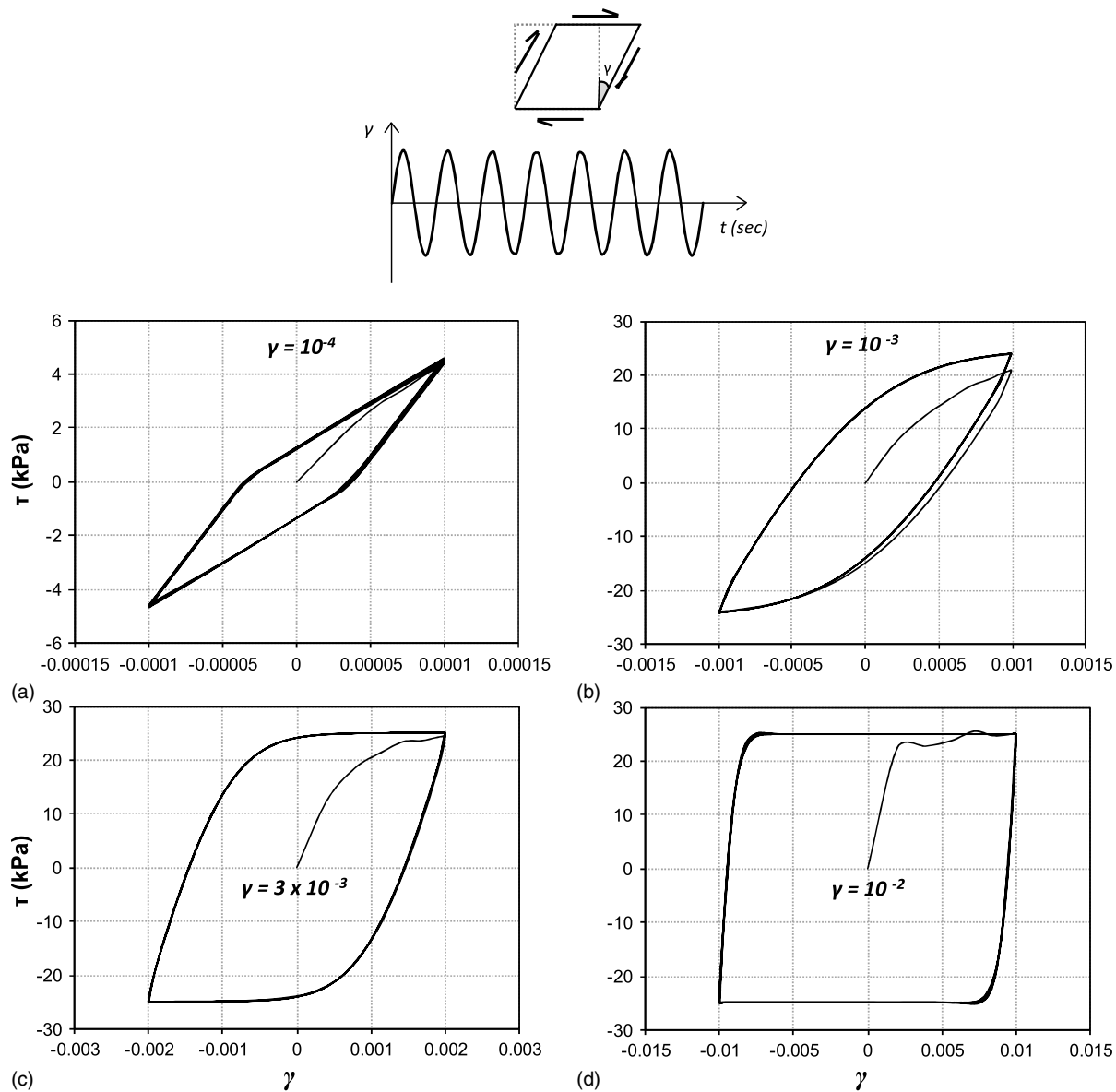
Fig. 5. FE simulation of simple shear test in sand ($\phi = 30°$, $G_o = 65$ MPa, $\sigma_{vo} = 50$ kPa). $\tau - \gamma$ hysteresis loops for different stain levels: (a) $\gamma = 10^{-4}$; (b) $\gamma = 10^{-3}$; (c) $\gamma = 3 \times 10^{-3}$; and (d) $\gamma = 10^{-2}$

Figs. 9–11 compare the FE-computed with the measured results in terms of (a) moment-rotation response and (b) settlement-rotation response of the foundation. More specifically,

First Loading Packet
Some uplifting can be traced in the moment-rotation loops predicted by the numerical model during the first loading packet [Fig. 9(a)], something not observed to the same extent in the experiment. The latter are indicative of increased plastic straining of the soil underneath the footing, hence resulting in higher dissipation of energy as elucidated by the area included within the experimental hysteresis loops. The analysis slightly overpredicts the maximum moment of the system during loading to the east direction (negative values in the diagram), whereas the discrepancy becomes larger in the opposite direction.

The experimentally measured hysteresis loops systematically reveal a rather rapid decrease of the moment (by about 30%) at every maximum moment attainment, which is not followed by a respective decrease in footing rotation (in both loading directions). This is clearly demonstrated by the almost vertical segments of the

loop immediately upon initiation of unloading and, in turn, results in substantial growth of the area of the M-θ loop. This may be the product of localized plastification underneath the footing edges, which could be attributed to reduced strength of the soil in these areas (a result of either previous cycles of shearing, soil inhomogeneities, or details of the experimental procedure, which are not precisely known and/or cannot be reproduced with the numerical model).

The model reliably reproduces the experimental settlement-rotation curve [Fig. 9(b)] both in terms of settlement per cycle and total settlement. Admittedly, however, apart from the general agreement, note that the numerical analysis predicts an uplifting-dominated response (indicated by the steep edges of the settlement-rotation plot) as opposed to the sinking-dominated response observed in the experiment. This discrepancy could also be attributed to localized plastification underneath the footing edges.

Second Loading Packet
During the second loading-unloading packet, both the experiment and the analysis show that a large area is enclosed within the
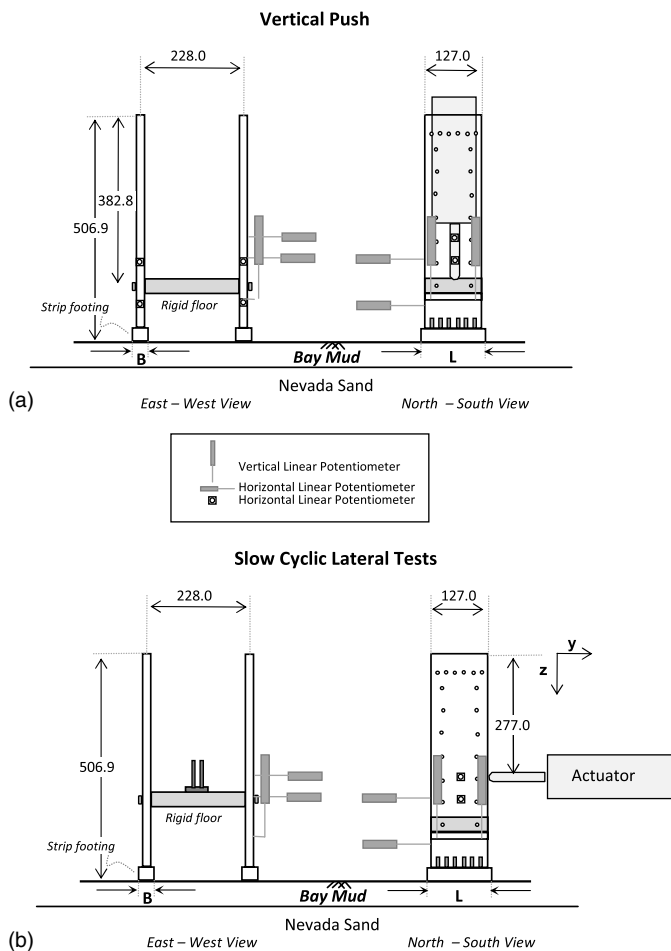
Fig. 6. Schematic of the general setup of the centrifuge experiments conducted at UC Davis (after Gajan et al. 2005): (a) vertical push (test KRR03-AW) configuration; (b) slow cyclic lateral push (test KRR03-AE); all units are in millimeters (model scale)

hysteresis loops [Fig. 10(a)], revealing the dissipation of a substantial amount of energy at the footing-soil interface. Experimental measurement and model prediction show that the ultimate moment capacity M_{ult} of the system has been attained. Its value is of the order of 300 kNm. The deviation of the experimental measurement from this value when the footing is loaded to the east (negative values) is tentatively attributed to some experimental asymmetry or, as before, soil inhomogeneity.

As shown in Fig. 10(b), with the exception of a slight underprediction of the settlement by the numerical analysis, the comparison in terms of settlement-rotation response is quite satisfactory.

Third Loading Packet
Excessive plastification is evident in both the experimental results and the numerical prediction [Fig. 11(a)]. The hysteresis loops reveal a highly nonlinear response of the system. The curve now conspicuously manifests the mobilization of the ultimate capacity ($M_{ult} \approx 300$ kNm): increase of rotation for constant moment. Still, the nonsymmetric behavior (different values of the ultimate moments in the east and west direction) demonstrated by the experimental curve cannot be precisely captured with the numerical analysis.

The numerical prediction is quite successful in terms of the settlement-rotation response [Fig. 11(b)]. According to Gajan et al. (2005), foundation rocking during large amplitude lateral loading leads to (permanent) loss of contact between the soil and
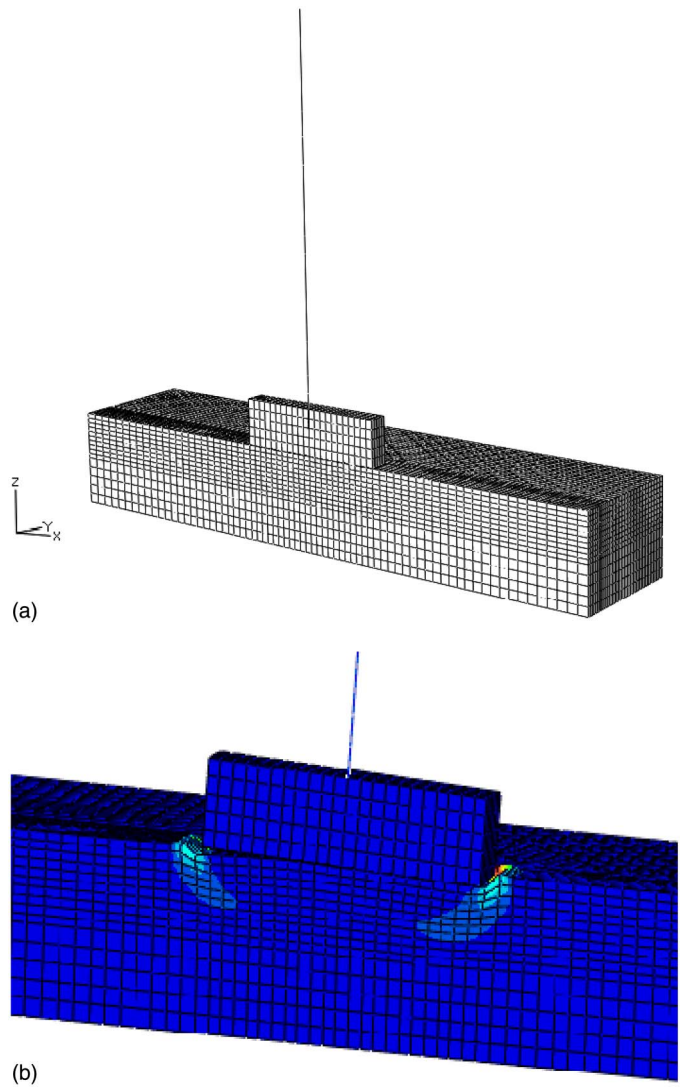

Fig. 7. (a) 3D finite-element half-model utilized for the numerical analyses of the UC Davis centrifuge experiments; (b) snapshot of deformed mesh with superimposed plastic strain contours; note the gap formation on the left side of the footing where it detaches from the underlying ground, and the plastic strain concentration at both edges

the footing. The generated gap at the uplifted side is associated with a drastic reduction of the effective width of the foundation, leading to extensive soil yielding at the opposite side, further increasing the detached area of the foundation [see also Fig. 7(b)]. This is clearly betrayed by the sharp edges of the settlement-rotation curves.

Generally, experiment and analysis confirm that the moment-rotation plot does not reveal any appreciable reduction in moment capacity with increasing number of cycles, or rotation amplitude, but it does demonstrate a degradation of rotational stiffness with increasing rotation amplitude. Moreover, the model realistically reproduces the accumulation of permanent settlement underneath the

Table 1. Constitutive Model Parameters Used in the Validation Tests

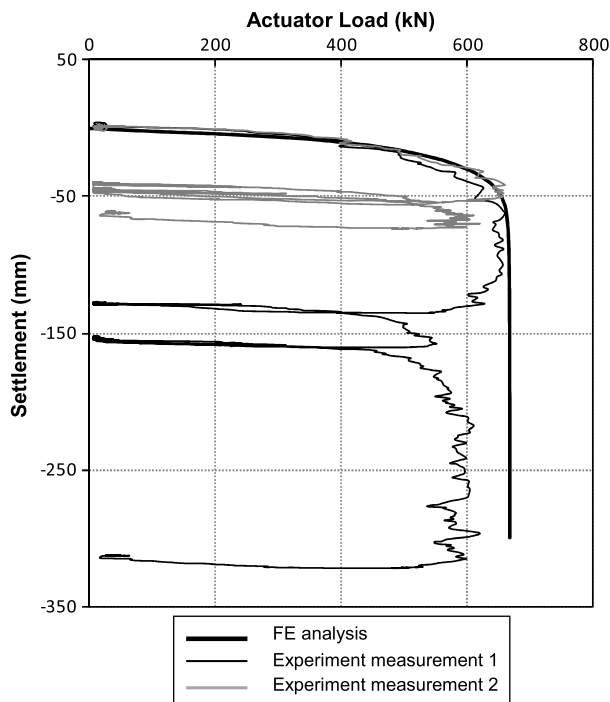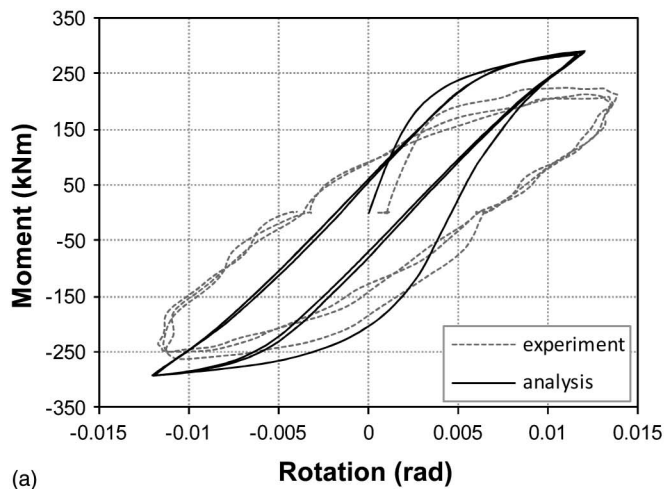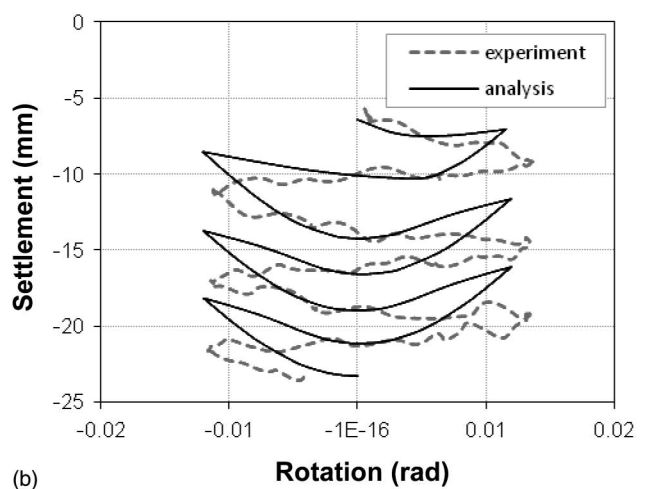| Test	Material	λ	a	S_u	ϕ (°)	v
UC Davis experiment	Clay	0.1	600	100	N/A	0.3
TRISEE experiment	Sand HD	0.1	8,500	N/A	43	0.3
	Sand LD − FS = 5	0.1	6,000	N/A	35	0.3
	Sand LD − FS = 5	0.1	6,000	N/A	30	0.3

Fig. 8. Model validation against UC Davis centrifuge tests: comparison of FE-computed with experimental load-displacement response for the vertical push test

footing. The analysis confirms the experimental conclusion that, as the number of cycles increases, the rate of increase in settlement per cycle of rotation decreases. This is normally attributed to the increase of soil vertical stiffness attributable to soil densification. However, as seen in the model description [Eqs. (4)–(10)], the model is not capable of reproducing such an increase in soil stiffness with settlement (i.e., the effect of soil densification). Nevertheless, as evidenced by the results, the systemic behavior is captured within acceptable engineering accuracy. This is attributed to the fact that as the footing settlement increases, soil plastification has to propagate deeper into the soil and, hence, an increasing number of elements must be contained within the failure mass. As the number of elements that must reach failure for the footing to settle

increases, the rate of settlement will unavoidably decrease. Hence, although at the element level the model is not capable of capturing dynamic densification effects, the systemic behavior is captured correctly. At least for the specific problem, such systemic effects are probably more important.

Although the model predicts the settlement quite accurately, the energy dissipation prediction is not as successful. As can be seen in the rotation-settlement plots of Figs. 9–11, the model tends to underpredict foundation uplifting as the loading packets increase. Although the total settlement is predicted with reasonable engineering accuracy, the settlement per loading cycle is underpredicted. For example [Fig. 11(b)], during the first cycle of the third packet the measured settlement (at the center of the footing) reduces from its initial value of −52 mm to about −28 mm because of uplifting. The numerical prediction is a mere −40 mm, which means that foundation uplifting is substantially underpredicted. The same observation applies to all subsequent loading cycles. This underprediction of uplifting, which is the main mechanism of energy dissipation in such systems (e.g., Housner 1963; Gottardi and Butterfield 1993; Gajan et al. 2003a; Gajan and Kutter 2008) apparently leads to the observed underprediction of energy dissipation. In contrast, as the model is able to correctly predict the soil ultimate strength [Fig. 11(a)], the total soil settlement is correctly predicted. Naturally, such effects are more obvious in the third loading packet, during which the uplifting is more intense.

Model Validation for Sand

We now proceed to validation of the simplified constitutive model for sand, making use of the TRISEE large-scale (1 g) geotechnical experiments conducted in ELSA facility in ISPRA, Italy.

Description of Tests

A series of slow cyclic and dynamic tests were performed on an isolated footing resting on saturated sand. Loading of the structure was stemming from the application of cycles of horizontal (shear) force and (overturning) moment simulating the inertial loading transmitted onto the foundation from the superstructure. The soil properties were varied to model a high density (HD) and a low density (LD) sand. The measured relative densities were $D_r = 85\%$ for the HD tests and $D_r = 45\%$ for the LD tests.
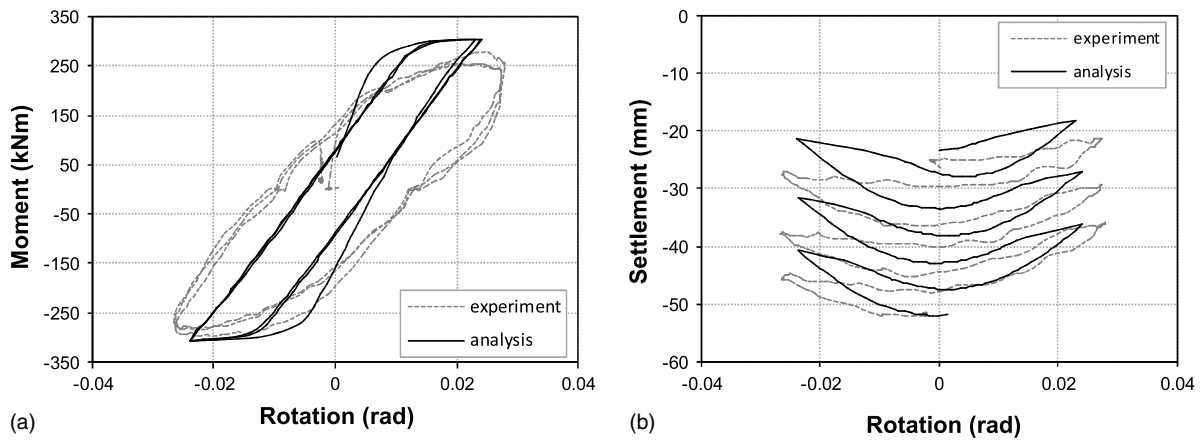

Fig. 9. Model validation against UC Davis centrifuge tests—first packet of loading; comparison of FE-computed with experimental (a) moment-rotation response; (b) settlement-rotation response

Fig. 10. Model validation against UC Davis centrifuge tests—second packet of loading; comparison of FE-computed with experimental (a) moment-rotation response; (b) settlement-rotation response
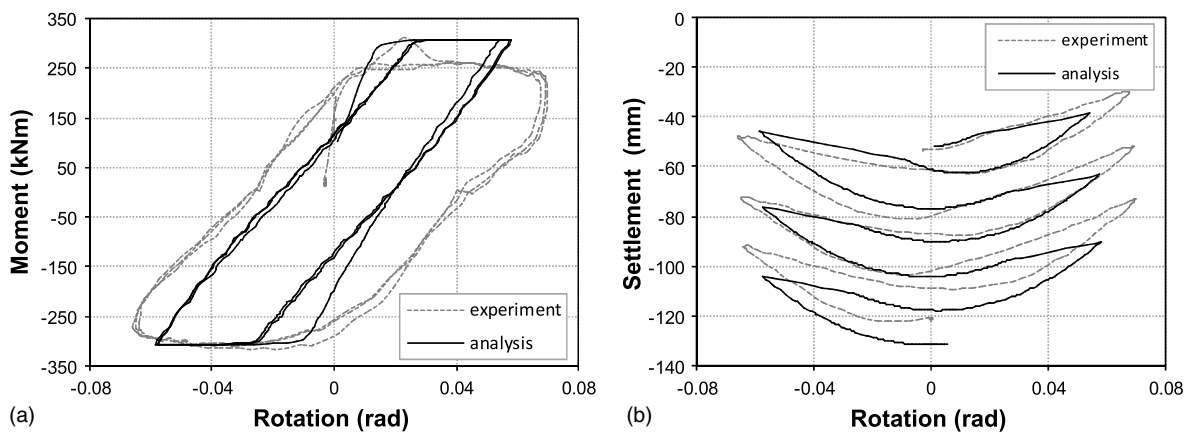

Fig. 11. Model validation against UC Davis centrifuge tests—third packet of loading; comparison of FE-computed with experimental (a) moment-rotation response; (b) settlement-rotation response

As schematically illustrated in Fig. 12 (after Faccioli et al. 1999), the experimental prototype consisted of a concrete caisson, filled with coarse-to-medium Ticino sand (Bellotti et al. 1996) and a rigid slab, representative of a typical concrete shallow footing. The sandbox dimensions were 4.6 by 4.6 m in plan and 4 m in height. The foundation was 1 m by 1 m in plan. The sandbox lateral boundaries were rigid and impermeable. Note that the response of the foundation may have been influenced by its proximity to the caisson lateral boundaries. The interface of the slab with the soil was made of concrete to achieve a high friction coefficient. The foundation was placed at 1 m depth in a trench of sand to obtain an overburden pressure of about 20 kPa; a 1 m high steel formwork was placed around the foundation to retain the sand.

An air cushion system transmitted a constant vertical load throughout the test. The design values for the vertical load were 300 kN and 100 kN for the HD and LD sand specimens, respectively (typical values of current design pressure levels for shallow foundations). In both cases, the design vertical load was considerably lower than the system's bearing-capacity. A hydraulic actuator set at 0.9 m above the foundation level for the HD case and at 0.935 m for the LD case was used to impose to the foundation the prescribed horizontal displacement time-history.

Before initiation of the slow cyclic tests, a vertical load (which was simulating the structure load and hence was maintained throughout the test) was applied on the foundation. This was followed by three series of horizontal slow cyclic loading (slow application of horizontal displacements), of which only the third one is being modeled in this paper. During the first phase, small-amplitude force-controlled cycles were applied to the structure. Phase II consisted of the application of a typical earthquake time-history providing a base shear similar to that of a four-story reinforced concrete building designed according to Eurocode 8.

During the third phase (which constitutes our validation target), the top of the structure was subjected to sine-shaped displacement cycles of increasing amplitude, until mobilization of the ultimate lateral foundation capacity. To achieve this capacity while avoiding excessive displacements, the test was displacement-controlled. The time-history of the applied horizontal displacement is displayed in Fig. 13 for the HD and the LD test. After application of the initial vertical loading, the settlement experienced by the foundation was around 7 mm for dense sand, and 16 mm for loose sand.

Numerical Analysis Methodology

The 3D FE model shown in Fig. 14 was developed to analyze the TRISEE experiment. The adopted numerical analysis methodology is the same as the one discussed in the previous section. The prescribed displacement was applied at the beam node at a height of 0.9 and 0.935 m above the foundation level for the HD and the LD tests, respectively. The part of the soil below the foundation level was saturated (degree of saturation ranging from 80–90%),
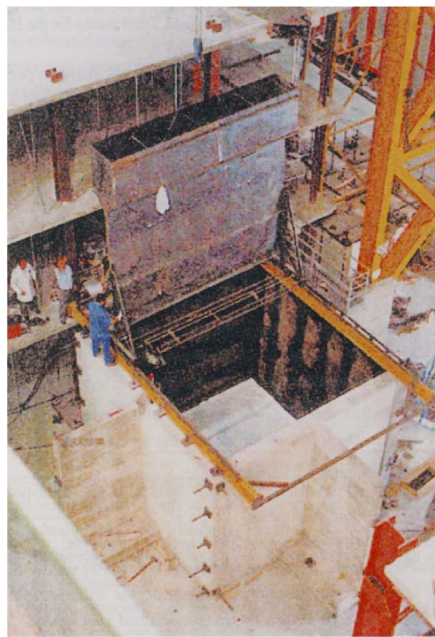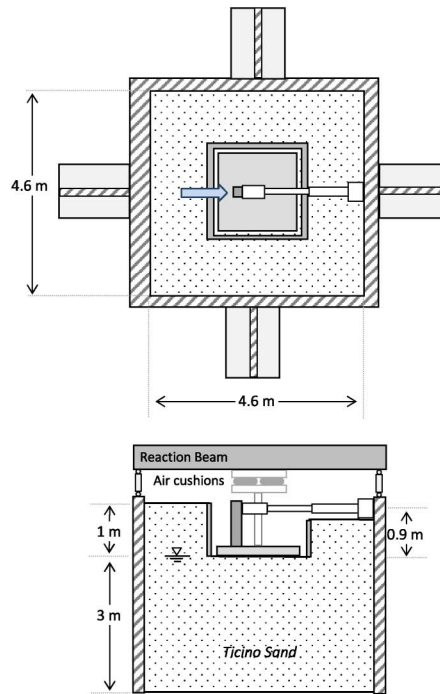
Fig. 12. TRISEE large-scale (1 g) experiment: (a) model and sand spreader; (b) schematic of the general experimental setup (after Faccioli et al. 1999)

whereas the overburden soil layers were dry. The two soil states were modeled assuming a different unit weight; while the overlying dry sand was modeled with its dry unit weight γ_{dry}, the saturated unit weight γ_{sat} was assumed for the saturated sand layer. This way, the effective stresses were taken into account in the analysis. It is noted that such analysis cannot possibly capture the development of transient pore pressure and its effect on soil response.

Similar to the tests on clay, initial sensitivity analyses were performed to calibrate the initial stiffness (parameter C of the constitutive model). The best match was achieved for $C = 8,500\sigma_y$ and $6,000\sigma_y$ for the HD and the LD tests, respectively (Table 1). A parabolic distribution of C with depth was assumed—a reasonable (but certainly not accurate) assumption for sand deposits. The initial

static factor of safety (FS_v) was not directly measured but has been calculated by various researchers (Negro et al. 2000; Faccioli et al. 2001; Kutter et al. 2003; Gajan et al. 2005). All researchers agree that the FS_v for the HD tests was about 5. This is consistent with the S-shaped $M\text{-}\theta$ curve of the HD test, as such a shape has been linked to intense uplifting of foundations (a characteristic of relatively high FS_v). Utilizing the strength parameters proposed by Belloti et al. (1998) and Ahmadi et al. (2005), for Ticino sand of $D_r = 85\%$ (peak friction angle $\varphi_p = 43$; constant volume friction angle $\varphi_{cv} = 35$), our analysis also produced an initial factor of safety $FS_v^{anal} \approx 5$. However, for the LD case, the FS_v as calculated by the aforementioned researchers ranges (astonishingly) from 2 to 7. Negro et al. (2000) report $FS_v = 5$ and Faccioli et al. (2001) estimated an $FS_v = 7$ on the basis of bearing-capacity formulas,
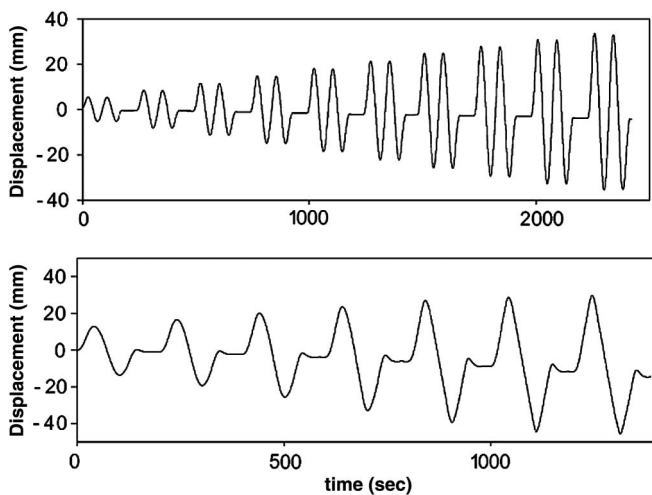

Fig. 13. TRISEE large-scale (1 g) experiment: time histories of imposed lateral displacement for (a) HD (high density) test (b) LD (low density) test
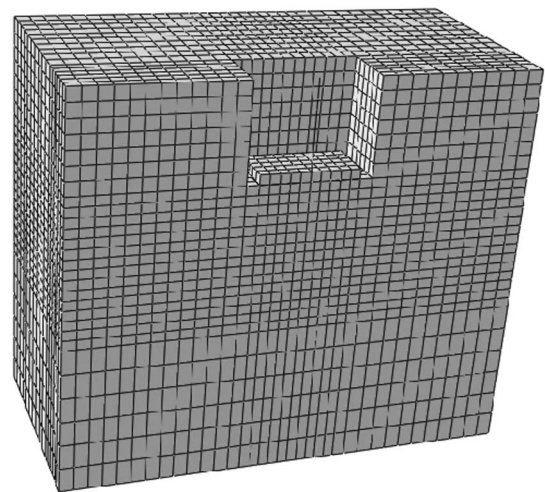

Fig. 14. 3D finite-element half-model utilized for numerical analyses of the TRISEE large-scale tests

with the theoretical strength of the Ticino sand. However, the oval shape of the LD M-θ curves is indeed a feature of low FS_v conditions (i.e., lower than 5). Allottey and El Naggar (2008) after back calculations of the FS_v on the basis of (a) moment capacity equations and (b) the Butterfield and Gottardi (1994) bounding surface, recommend that the actual factor of safety for the specific LD tests ranges between 2 and 2.85. Therefore, two strength scenaria are considered in our calculations, taking account of the Allottey and El Naggar (2008) recommendation that the peak friction angle of the Ticino sand achieved in the LD experiment ranges between 30 and 35°:

a. The $FS_v \approx 5$ scenario, assuming $\varphi_p = 35°$, and
b. The $FS_v \approx 3$ scenario, assuming $\varphi_p = 30°$.

Comparison of Numerical Predictions with Experimental Results

Dense Sand (HD Test)
A remarkable agreement is observed between the measured and the calculated hysteresis loops produced during slow cyclic tests [Fig. 15(a)]. Both loops evolve quite symmetrically. The numerical analysis effectively reproduces the lateral capacity of the system: $M_{ult} \approx 100$ kNm. The analysis captures with sufficient accuracy both the initial stiffness of the system and the gradual degradation of rotational stiffness with increasing rotation amplitude. Analysis and experiment produce an S-shaped moment-rotation curve, which clearly manifests an uplifting-dominated response. As the amplitude of imposed rotation increases, the numerical model slightly overpredicts the dissipation of energy during cyclic loading.

A relatively good agreement between the numerical prediction and the experiment is also achieved in terms of horizontal force versus horizontal displacement of the footing [Fig. 15(b)]. The experimental loop (dashed line) is slightly asymmetric, in that the maximum horizontal displacement is rather higher in the negative direction (6 mm) compared with that in the positive direction (5 mm). The numerically calculated loop (solid line), despite capturing the observed behavior, does not accurately predict the higher displacement in the negative direction ($\delta^{anal} = 5.5$ cm).

Loose Sand (LD Test)
Contrary to the uplifting behavior of the footing on HD sand, the foundation on loose sand is obviously subjected to substantial irrecoverable sinking within the soil. This is justified by both the numerical model and the experimental results, which show clearly larger energy dissipation in the loose sand for both FS_v scenarios (Fig. 16 for the $FS_v \approx 3$ scenario and Fig. 17 for the $FS_v \approx 5$ scenario). The loops produced during the LD tests are obviously asymmetric because of the irregularity of the input displacement time-history that contained a permanent negative horizontal displacement. The analysis did not capture this intense irregularity. Still a very good agreement is observed between the measured and the calculated hysteresis loops for the low $FS_v \approx 3$ scenario, whereas in the high $FS_v \approx 5$ case, the hysteresis exhibits moderately S-shaped loops, which are (as already discussed) indicative of uplifting. Both the initial stiffness of the system, as well as its stiffness during loading are successfully predicted. However, for the higher amplitudes of rotation, both scenarios predict a stiffer behavior.

The analysis has been successful in simulating the experimentally observed mobilization of the foundation capacity. In very good accord with the measured value, the predicted ultimate moment of the system is $M_{ult} \approx 40$ kNm in the negative loading direction. However, the $\varphi = 35°$ scenario leads to overestimation of the calculated moment capacity, whereas for the $\varphi = 30°$ case the capacity is rather accurately predicted.

Fig. 15. Model validation against the TRISEE large-scale tests; comparison of numerical analysis prediction (solid black line) with experimental result (dashed line) for the HD test: (a) Moment-rotation response; (b) lateral force-displacement response
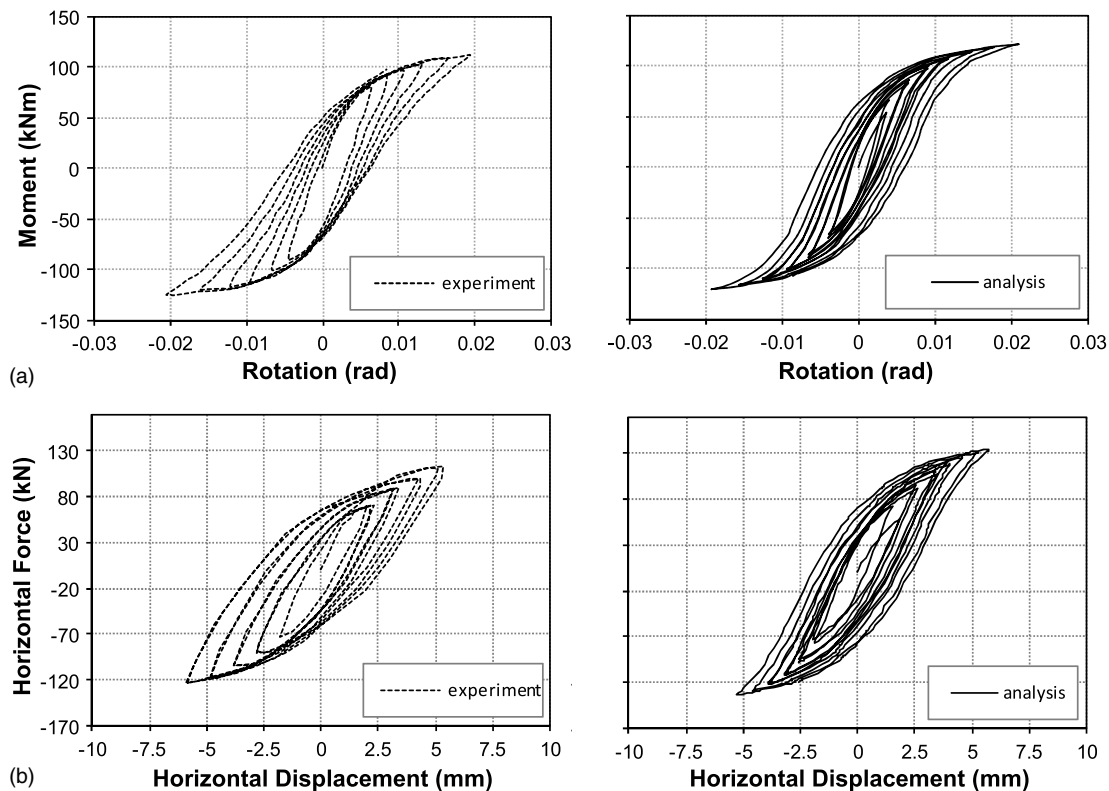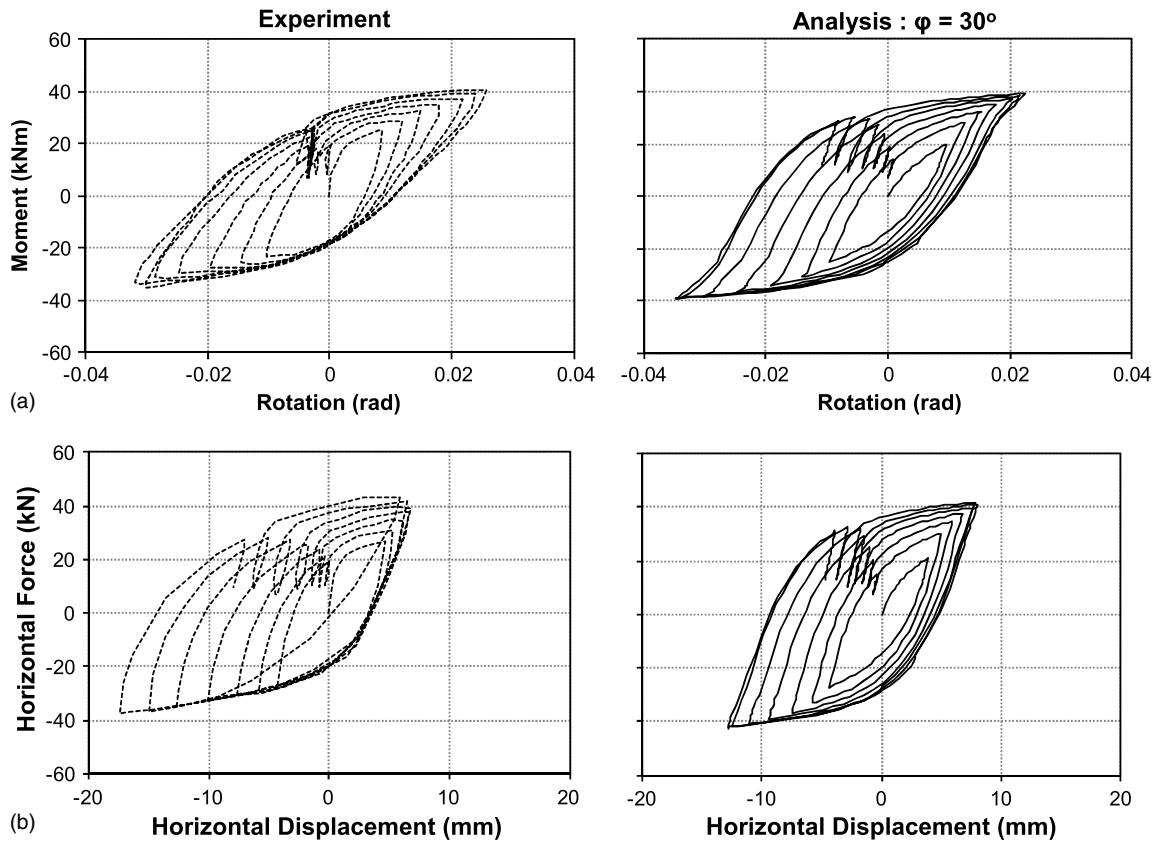
Fig. 16. Model validation against the TRISEE large-scale tests; comparison of numerical analysis prediction (solid black line) with experimental results (dashed line) for the LD test for the $FS_v \approx 3 - \varphi = 30°$ scenario: (a) moment-rotation response; (b) lateral force-displacement response
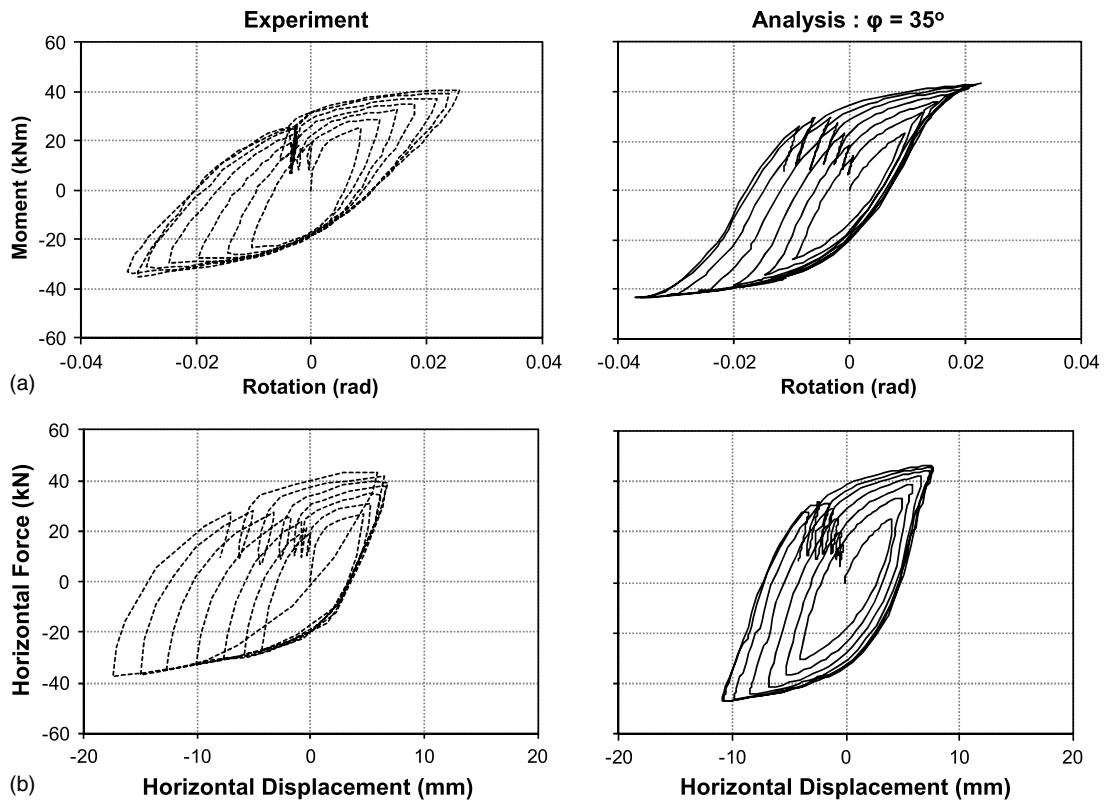

Fig. 17. Model validation against the TRISEE large-scale tests; comparison of numerical analysis prediction (solid black line) with experimental results (dashed line) for the LD test for the $FS_v \approx 5 - \varphi = 35°$ scenario: (a) moment-rotation response; (b) lateral force-displacement response

In terms of horizontal force versus horizontal displacement, the $\varphi = 30°$ scenario predicts lager displacements than the $\varphi = 35°$ case. Admittedly, however, none of the two scenarios are capable of capturing the intensity of asymmetric sliding (toward the negative *x*-axis direction).

Cyclic Foundation Settlement (HD and LD Test)

The comparison of the evolution of vertical displacements for the HD and LD tests is displayed in Fig. 18. *The recorded trend is almost linear in both cases, probably because of the progressive squeezing of sand underneath the plate toward the sides during the sinking of the foundation* (as suggested by Faccioli et al. 2001).

In all cases, settlements are accumulated underneath the footing, reaching ultimate values of about 20 mm and 70 mm for dense and loose sand, respectively. These values are slightly overpredicted by the analysis for the HD test: $s^{anal} = 25$ mm. While a cumulative settlement trend is macroscopically obvious in the HD case, the footing undergoes reversible settlement-uplifting cycles within each set of loading-unloading series. The numerical model indeed predicts the general trend, and it matches the seesawing shape of

settlement-uplifting cycles during each series [Fig. 18(b)], but results in (slightly) higher settlement.

For the LD case [Fig. 18(c)], both scenarios lead to reasonable predictions of the settlement: 59 mm for the $FS_v \approx 5$ scenario; 84 mm for the $FS_v \approx 3$ scenario. The predicted evolution of cyclic foundation settlement agrees reasonably with the experimental measurements. Observe that during the final stages of the LD test, the vertical displacements reveal some uplifting of the foundation; this is effectively captured by the numerical model when the $FS_v \approx 5$ scenario is considered ($\varphi = 35°$).

Summary and Conclusions

This paper has presented a simplified but fairly comprehensive constitutive model of clay and sand for analyzing the cyclic response of shallow foundations undergoing strong rocking oscillations, involving uplifting and mobilization of bearing-capacity "failure" mechanisms. Having as a basis a simple kinematic hardening constitutive model, readily available in commercial FE codes, a simple modification was implemented to render the model applicable for sand. The model was encoded in ABAQUS through a rather simple user subroutine, and thoroughly validated against centrifuge (UC Davis) and large-scale 1-g (TRISEE) experimental results.

The key conclusions and limitations can be summarized as follows.

1. The Von Mises failure criterion of the constitutive model can be considered appropriate for clay under undrained conditions. Phenomena such as pore-pressure buildup and dissipation cannot be captured. For the key aspects of the problem investigated herein, given the rapid application of seismic loading, undrained behavior is considered a reasonable simplification of reality.

2. The extended normal-pressure-dependent Von Mises failure criterion, employed to render the model applicable to sand, constitutes a simplified approximation of real sand behavior. By no means, can it be considered accurate or rigorous. The assumption of an associated plastic flow rule is also a "gross" simplification not valid for sand, the volumetric behavior of which largely depends on dilation. Hence, the volumetric behavior of sand cannot be reproduced.

3. Despite the above drawbacks, for the problem of interest (i.e., the nonlinear response of shallow foundations) the proposed simplified model has been shown to yield quite reasonable results. Through the validation presented herein, the model was found capable of capturing with reasonable engineering accuracy
   - The response of shallow foundations subjected to vertical loading, both in terms of FS_v and load-settlement response,
   - The lateral capacity of the shallow foundations, as expressed through M_{ult},
   - The lateral cyclic performance of the foundation, both in terms of moment-rotation and load-displacement response, and
   - The accumulation of foundation settlement resulting from lateral cyclic loading.

4. Some discrepancies (small in general) between numerical predictions and experimental results can be attributed to the approximate nature of the model, and several experimental details (such as the exact strength and stiffness profiles, soil inhomogeneities, slight but possibly important asymmetries, and so forth) that are either unknown or cannot be captured numerically.
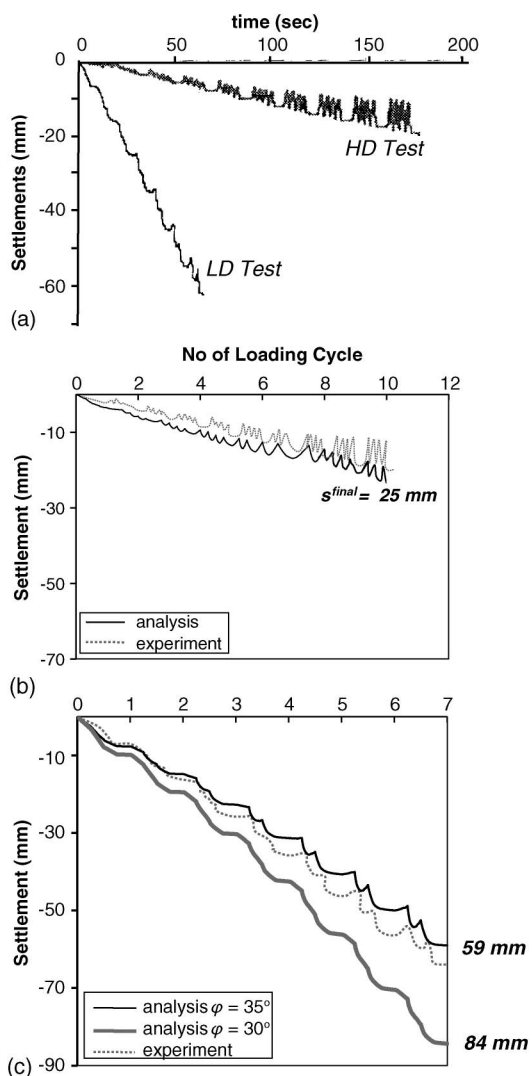

Fig. 18. Model validation against the TRISEE large-scale tests: (a) experimentally measured evolution of foundation cyclic settlement; comparison of numerical prediction with experimental results for (b) HD test; (c) LD test (for both scenarios)

5. Having knowledge of soil strength (S_u for clay and φ for sand) and small-strain stiffness (G_o or V_s), the model requires calibration of only two parameters (λ and ratio a), which has been shown to be simple and straightforward: it is conducted on the basis of G-γ curves.

6. Easily implemented in commercial FE codes (as done here through a simple user subroutine in ABAQUS), the model is believed to provide a practically applicable solution not restricted to simple superstructures, and not to be solely used by numerical analysis specialists.

Acknowledgments

References

ABAQUS [Computer software]. ABAQUS, Inc., Providence, RI.

Ahmadi, M. M., Byrne, P. M., and Campanella, R. G. (2005). "Cone trip resistance in sand: modeling, verification, and applications." *Can. Geotech. J.*, 42(4), 977–993.

Allotey, N., and El Naggar, M. H. (2003). "Analytical moment—rotation curves for rigid foundations based on a Winkler model." *Soil Dyn. Earthquake Eng.*, 23(5), 367–381.

Allotey, N. K., and El Naggar, M. H. (2008). "An investigation into the Winkler modeling of the cyclic response of rigid footings." *Soil Dyn. Earthquake Eng.*, 28(1), 44–57.

Anastasopoulos, I., Gazetas, G., Loli, M., Apostolou, M, and Gerolymos, N. (2009). "Soil failure can be used for seismic protection of structures." *Bull. Earthquake Eng.*, 8, (2), 309–326.

Armstrong, P. J., and Frederick, C. O. (1966). "A mathematical representation of the multiaxial bauschinger effect." *CEGB Rep. No. RD/B/N 731*.

Bartlett, P. (1979). "Foundation rocking on a clay soil." M.E. thesis, Univ. of Auckland, New Zealand.

Bellotti, R., Crippa, V., Pedroni, S., and Ghionna, V. N. (1998). "Saturation of sand specimen for calibration chamber tests." *Proc., 1st Int. Symp. on Penetration Testing (ISOPT-1)*, Vol. 2, J. DeRuiter, ed., A. A. Balkema, Rotterdam, Netherlands, 661–671.

Bellotti, R., Jamiolkowski, M., Lo Presti, D., and O'Neil, D. (1996). "Anisotropy of small strain stiffness in Ticino sand." *Géotechnique*, 46(1), 115–131.

Butterfield, R., and Gottardi, G. (1994). "A complete three-dimensional failure envelope for shallow footings on sand." *Géotechnique*, 44(1), 181–184.

Chatzigogos, C. T., Pecker, A., and Salencon, J. (2009). "Macroelement modeling of shallow foundations." *Soil Dyn. Earthquake Eng.*, 29(5), 765–781.

Comartin, C. D., Niewiaroski, R. W., Freeman, S., and Turner, F. M. (2000). "Seismic evaluation and retrofit of concrete buildings: a practical overview of the ATC-40 document." *Earthquake Spectra*, 16(1), 241–262.

Cremer, C., Pecker, A., and Davenne, L. (2001). "Cyclic macro-element for soil-structure interaction: material and geometrical non-linearities." *Int. J. Numer. Anal. Methods Geomech.*, 25(13), 1257–1284.

Cremer, C., Pecker, A., and Davenne, L. (2002). "Modelling of nonlinear dynamic behaviour of a shallow strip foundation with macro-element." *J. Earthquake Eng.*, 6(2), 175–211.

Dafalias, Y. F. (1986). "An anisotropic critical state soil plasticity model." *Mech. Res. Commun.*, 13(6), 341–347.

Dafalias, Y. F., and Manzari, M. T. (2004). "Simple plasticity sand model accounting for fabric change effects." *J. Eng. Mech.*, 130(6), 622–634.

Einav, I., Puzrin, A. M., and Houlsby, G. T. (2003). "Continuous hyperplastic models for overconsolidated clays." *Math. Comput. Model.*, 37(5/6), 515–523.

Faccioli, E., Paolucci, R., and Vanini, M., eds. (1999). *TRISEE: 3D site effects and soil-foundation interaction in earthquake and vibration risk evaluation*, European Commission Publications.

Faccioli, E., Paolucci, R., and Vivero, G. (2001). "Investigation of seismic soil-footing interaction by large scale cyclic tests and analytical models." *Proc. 4th Int. Conf. on Recent Advances in Geotechnical Earthquake Engineering and Soil Dynamics*, S. Prakash, ed., Missouri Univ. of Science and Technology, Rolla, MO.

FEMA. (2000). "Prestandard and commentary for the seismic rehabilitation of buildings." *FEMA 356*, Washington, DC.

Gajan, S., and Kutter, B. L. (2008). "Capacity, settlement, and energy dissipation of shallow footings subjected to rocking." *J. Geotech. Geoenviron. Eng.*, 134(8), 1129–1141.

Gajan, S., Kutter, B. L., Phalen, J. D., Hutchinson, T. C., and Martin, G. R. (2005). "Centrifuge modeling of load-deformation behavior of rocking shallow foundations." *Soil Dyn. Earthquake Eng.*, 25(7-10), 773–783.

Gajan, S., Phalen, J. D., and Kutter, B. L. (2003a). "Soil-foundation-structure interaction: Shallow foundations. Centrifuge data report for test series SSG02." *Rep. No. UCD/CGMDR-03/01*, Univ. of California, Davis, CA.

Gajan, S., Phalen, J. D., and Kutter, B. L. (2003b). "Soil-foundation-structure interaction: shallow foundations. Centrifuge data report for test series SSG03." *Rep. No.UCD/CGMDR-03/02*, Univ of California, Davis, CA.

Gajo, A., and Muir Wood, D. A. (1999). "Kinematic hardening constitutive model for sands: A multiaxial formulation." *Int. J. Numer. Anal. Meth. Geomech.*, 23(9), 925–965.

Gazetas, G., Anastasopoulos, I., and Apostolou, M. (2007). "Shallow and deep foundations under fault rupture or strong seismic shaking." *Earthquake geotechnical engineering*, K. Pitilakis, ed., Vol. 6, Springer, Berlin, 185–210.

Gazetas, G., Apostolou, M., and Anastasopoulos, I. (2003). "Seismic uplifting of foundations on soft soil, with examples from Adapazari (Izmit 1999, Earthquake)." *BGA Int. Conf. on Foundation Innovations, Observations, Design & Practice*, Univ. of Dundee, Scotland, 37–50.

Georgiadis, M., and Butterfield, R. (1988). "Displacements of footings on sand under eccentric and inclined loads." *Can. Geotech. J.*, 25(2), pp. 199–212.

Gerolymos, N., Gazetas, G., and Tazoh, T. (2005). "Seismic response of yielding pile in non-linear soil." *Proc. 1st Greece-Japan Workshop, Seismic Design, Observation, and Retrofit of Foundations*, National Technical Univ. of Athens, Athens, Greece, 25–36.

Gottardi, G., and Butterfield, R. (1993). "On the bearing capacity of surface footings on sand under general planar loads." *Soils Found.*, 33(3), 68–79.

Harden, C. W., and Hutchinson, T. C. (2009). "Beam-on-nonlinear-winkler foundation modeling of shallow, rocking-dominated footings." *Earthquake Spectra*, 25(2), 277–300.

Harden, C. W., Hutchinson, T. C., Martin, G. R., and Kutter, B. L. (2005). "Numerical modeling of the nonlinear cyclic response of shallow foundations." *Rep. No. PEER-2005/04*, Pacific Earthquake Engineering Research Center, University of California, Berkeley, CA.

Hardin, B. O., and Richart, F. E. Jr. (1963). "Elastic wave velocities in granular soils." *J. Soil Mech. Found. Div.*, 89(1), 33–66.

Houlsby, G. T. (1986). "A general failure criterion for frictional and cohesive materials." *Soils Found.*, 26(2), 97–101.

Houlsby, G. T., and Puzrin, A. M. (1999). "The bearing capacity of a strip footing on clay under combined loading." *Proc. R. Soc. London, Ser. A*, 455(1983), 893–916.

Houlsby, G. T., and Puzrin, A. M. (2006). *Principles of hyperplasticity*, Springer, Berlin.

Housner, G. W. (1963). "The behavior of inverted pendulum structures during earthquakes." *Bull. Seismol. Soc. Am.*, 53(2), 403–417.

Ishibashi, I., and Zhang, X. (1993). "Unified dynamic shear moduli and damping ratios of sand and clay." *Soils Found.*, 33(1), 182.

Jefferies, M. G. (1993). "Nor-sand: A simple critical state model for sand." *Géotechnique*, 43(1), 91–103.

Jeremic, B., Runesson, K., and Sture, S. (1999). "A model for elastic-plastic pressure sensitive materials subjected to large deformations." *Int. J. Solids Struct.*, 36(31/32), 4901–4918.

Kawashima, K., Nagai, T., and Sakellaraki, D. (2007). "Rocking seismic isolation of bridges supported by spread foundations." *Proc. of 2nd Japan-Greece Workshop on Seismic Design, Observation, and Retrofit of Foundations*, Japan Society of Civil Engineers, Tokyo, 254–265.

Kutter, B. L. (1995). "Recent advances in centrifuge modeling of seismic shaking, Proceedings." *3rd Int. Conf. on Recent Advances in Geotechnical Earthquake Engineering and Soil Dynamics*, Vol. II, Missouri Univ. of Science and Technology, Rolla, MO, 927–941.

Kutter, B. L., Martin, G., Hutchinson, T. C., Harden, C., Gajan, S., and Phalen, J. D. (2003). *Status report on study of modeling of nonlinear cyclic load—Deformation behavior of shallow foundations*, Univ. of California, Davis, CA, PEER Workshop.

Lemaitre, J., and Chaboche, J.-L.(1990). *Mechanics of solid materials*, Cambridge Univ. Press, Cambridge, UK.

Le Pape, Y., and Sieffert, J. P. (2001). "Application of thermodynamics to the global modelling of shallow foundations on frictional material." *Int. J. Numer. Anal. Methods Geomech.*, 25(14), 1377–1408.

Makris, N., and Roussos, Y. S. (2000). "Rocking response of rigid blocks under near-source ground motions." *Géotechnique*, 50(3), 243–262.

Martin, G. R., and Lam, I. P. (2000). "Earthquake resistant design of foundations: Retrofit of existing foundations." *Proc., GeoEng 2000 Conf.*, GeoEng2000, Melbourne, Australia.

Mayne, P. W., and Rix, G. J. (1993). "$G_{max} - q_c$ relationships for clays." *Geotech. Test. J.*, 16(1), 54–60.

Negro, P., Paolucci, R., Pedretti, S., and Faccioli, E. (2000). "Large scale soil-structure interaction experiments on sand under cyclic load." *Proc., 12th World Conf. on Earthquake Engineering*, Paper No. 1191, New Zealand Society for Earthquake Engineering, Silverstream, Upper Hutt, New Zealand.

Paolucci, R. (1997). "Simplified evaluation of earthquake induced permanent displacements of shallow foundations." *J. Earthquake Eng.*, 1(3), 563–579.

Paolucci, R., Shirato, M., and Yilmaz, M. T. (2008). "Seismic behaviour of shallow foundations: Shaking table experiments vs numerical modelling." *Earthquake Eng. Struct. Dyn.*, 37(4), 577–595.

Pecker, A. (1998). "Capacity design principles for shallow foundations in seismic areas." *Proc. 11th European Conf. on Earthquake Engineering*, A. A. Balkema, Rotterdam, Netherlands.

Pecker, A. (2002). "Earthquake resistant design of shallow foundations." *Recent advances in earthquake geotechnical engineering and microzonation*, A. Ansal, ed., Springer, Netherlands.

Pecker, A. (2003). "Aseismic foundation design process, lessons learned from two major projects: the Vasco de Gama and the Rion Antirion bridges." *ACI Int. Conf. on Seismic Bridge Design and Retrofit*, Univ. of California, San Diego, La Jolla, CA.

Pecker, A. (2005). "Design and construction of the foundations of the Rion-Antirion Bridge." *Proc., 1st Greece Japan Workshop on Seismic Design, Observation, and Retrofit of Foundations*, G. Gazetas and T. Tazoh, eds., National Technical Univ. of Athens, Athens, Greece, 119–130.

Pecker, A., and Pender, M. J. (2000). "Earthquake resistant design of foundations: New construction." *Proc., GeoEng2000*, Melbourne, Australia, 313–332.

Pender, M. J. (2007). "Seismic design and performance of surface foundations." *Earthquake geotechnical engineering*, K. Pitilakis, ed., Vol. 6, Springer, Berlin, 217–243.

Pestana, J. M. (1994). "A unified constitutive model for clays and sands." Sc.D. thesis, Dept. of Civil and Environmental Engineering, Massachusetts Institute of Technology, Cambridge, MA.

Pestana, J. M., and Whittle, A. J. (1995). "Compression model for cohessionless soils." *Géotechnique*, 45(4), 611–631.

Pestana, J. M., and Whittle, A. J. (1999). "Formulation of a unified constitutive model for clays and sands." *Int. J. Numer. Anal. Methods Geomech.*, 23(12), 1215–1243.

Phalen, J. D. (2003). "Physical modeling of the soil-foundation interaction of spread footings subjected to lateral cyclic loading." M.S. thesis, School of Engineering, Univ. of California, Davis, CA.

Prandtl, L. (1921). "Uber die eindringungsfestigkeit (harte) plastischer baustoffe und die festigkeit von schneiden." *Zeitschrift fur angewandte Mathematik und Mechanik*, 1(1), 15–20.

Prévost, J. H. (1980). "Mechanics of continuous porous media." *Int. J. Eng. Sci.*, 18(6), 787–800.

Puzrin, A. M., and Houlsby, G. T. (2001a). "Strain-based plasticity models for soils and the BRICK model as an example of the hyperplasticity approach." *Géotechnique*, 51(2), 169–172.

Puzrin, A. M., and Houlsby, G. T. (2001b). "Fundamentals of kinematic hardening hyperplasticity." *Int. J. Solids Struct.*, 38(21), 3771–3794.

Puzrin, A. M., and Houlsby, G. T. (2001c). "On the non-intersection dilemma in multi-surface plasticity." *Géotechnique*, 51(4), 369–372.

Robertson, P. K., and Campanella, R. G. (1983a). "Interpretation of cone penetration tests—Part I (sand)." *Can. Geotech. J.*, 20(4), 718–733.

Robertson, P. K., and Campanella, R. G. (1983b). "Interpretation of cone penetration tests—Part II (clay)." *Can. Geotech. J.*, 20(4), 734–745.

Rosebrook, K. R., and Kutter, B. L. (2001a). "Soil-foundation-structure interaction: shallow foundations. Centrifuge Data Report for test series KRR01." *Rep. No. UCD/CGMDR-01/09*, Univ. of California, Davis, CA.

Rosebrook, K. R., and Kutter, B. L. (2001b). "Soil-foundation-structure interaction: shallow foundations. Centrifuge Data Report for test series KRR03." *Rep. No. UCD/CGMDR-01/11*, Univ. of California, Davis, CA.

Rosebrook, K. R., and Kutter, B. L. (2001c). "Soil-foundation-structure interaction: shallow foundations. Centrifuge Data Report for test series KRR02." *Rep. No. UCD/CGMDR-01/10*, Univ. of California, Davis, CA.

Seed, H. B., Wong, R. T., Idriss, I. M., and Tokimatsu, K. (1986). "Moduli and damping factors for dynamic analyses of cohesionless soils." *J. Soil Mech. Found., Div.*, 112(11), 1016–1032.

Taylor, P. W., Bartlett, P. E., and Wiessing, P. R. (1981). "Foundation rocking under earthquake loading." *Proc., 10th Int. Conf. on Soil Mechanics and Foundation Engineering*, A. A. Balkema, Stockholm, Sweden, 3, 313–322.

Vucetic, M., and Dobry, R. (1991). "Effect of soil plasticity on cyclic response." *J. Geotech. Eng.*, 117(1), 89–107.

Ziegler, H. (1959). "A modification of Prager's hardening rule." *Quart. Appl. Math.*, 17, 55–65.